

Turbulent Flow of Non-Newtonian Fluids in a Partially Blocked Pipe

J. Singh¹, M. Rudman¹, H.M. Blackburn¹, A. Chryss² and L. Pullum²

¹Department of Mechanical and Aerospace Engineering
 Monash University, Clayton, VIC 3800, Australia

²CSIRO Mineral Resources Flagship
 Clayton, VIC 3168, Australia

Abstract

Fine particle suspensions often form non-Newtonian slurries. In mining applications these suspensions can also transport coarse particles that can form a settled bed on the bottom of the pipe. These settled solid particles can be stationary or move as a bed, depending on the flow conditions. In this study, direct numerical simulation is carried out treating the fine particle suspensions as homogeneous yield pseudo-plastic fluid i.e. shear-thinning fluid with yield stress. Flow through a full circular pipe as well as through partially blocked pipes for two different bed depths are considered. Results are presented for flow with stationary and moving beds. For stationary bed cases, results are compared with Newtonian fluid flow results. In all simulations, flows are assumed to be driven by a constant axial pressure gradient. Results show that non-Newtonian fluid flows are more sensitive to change in the bed depth and the bed acts as a damper to turbulent fluctuations.

Introduction

Hydraulic transport of fine particle slurries through pipeline is very common in mining and other industries. These slurries usually show non-Newtonian behaviour. A range of different types of non-Newtonian fluids exists but they can be broadly categorised as time-independent (also called generalized non-Newtonian or GN fluids) and time-dependent non-Newtonian fluids. Visco-elastic non-Newtonian fluids, which are the subset of time-dependent non-Newtonian fluids, have attracted many studies due to their turbulent drag reduction property. However, Bird et al. [1] observed that the rheology of most non-Newtonian fluids found in industry is primarily time-independent in nature with negligible visco-elastic effects.

For GN fluids, relation between shear stress can be defined as a function of second invariant of strain rate tensor i.e.

$$\tau = \tau(\dot{\gamma}) \quad \dot{\gamma} = \sqrt{2S_{ij}S_{ij}} \quad S_{ij} = \frac{1}{2} \left(\frac{\partial u_i}{\partial x_j} + \frac{\partial u_j}{\partial x_i} \right) \quad (1)$$

Effective viscosity (sometimes called apparent viscosity) is calculated as:

$$\eta_a = \tau / \dot{\gamma} \quad (2)$$

The relation between shear stress and shear rate is described by a rheology model, the parameters of which are usually determined by data fitting to rheometry measurements. Once the rheology model is fixed, it is usually possible to solve for the laminar flow of these GN fluids analytically. However, even for quite viscous fluids, it is possible that their flow can be transitional or turbulent and such flows are too complex to solve analytically even for Newtonian fluids. For non-Newtonian fluid flows this becomes more intractable due to added difficulties of a more complex rheology.

Fine particle slurries in the mining and waste disposal industries often characterized as GN fluid with yield. In the pipeline flow of water where the fluid viscosity is low, the main mechanism to keep fine particles in suspension is turbulence and inter-particle interactions. Therefore in laminar flow of water and even in turbulent flow where turbulent intensities are not high enough, solid coarse particles have a tendency to settle down and form a bed. This causes partial blockage of the pipe. However, when fine solid particles are mixed in water with sufficiently high concentration, fine particle slurries are produced which show complex rheological behaviour (non-Newtonian behaviour). The viscosity of these fine particle slurries is usually quite high. A higher viscosity of these slurries (along with yield stress) acts to keep the particles in suspension and more distributed even for a low flow rates at which the particles in water exhibit a greater settling trend [2]. In turbulent flow of fine particles slurries, the flow may pick-up heavier coarse particles by the action of turbulence. Mechanisms of holding particles in turbulent flow depend on the turbulent intensities working against gravity. If the turbulent intensities are not strong enough, particles will settle down causing a reduction in area available for flow and hence changing the geometry. Change in geometry induces secondary flows. For suspensions with particles much smaller than the conduit size, the secondary flows can be the dominant mechanism for shear-induced enhancement of particle suspension [2, 3]. Modelling of flow with solid particles is quite expensive but by understanding the change in turbulent characteristics due to the change in flow area an estimate of the fate of suspension of coarse solid particles can be made.

Rigorous experimental measurements in slurry flows are very difficult, especially where the concentration is sufficiently high to produce non-Newtonian effects. Experimental studies with other non-Newtonian fluids which are optically clear have their own limitations such as carboxymethyl-cellulose (CMC), which shows visco-elasticity at high shear rates. Also the rheology parameters of non-Newtonian fluids are interdependent. In practice, it is very difficult to isolate the effect of one rheology parameter from others.

Numerical studies of flow of GN fluids, especially using direct numerical simulation (DNS), have shown significant promise in helping to understand the flow behaviour in transition and turbulence region [4]. The main benefit of using a DNS technique is that once validated, it can be reliably used to model the flow behaviour and provide a detailed picture of turbulent structure. In addition, it also has advantages of numerical modelling where rheology effects such as visco-elasticity can be excluded from the model and effect of different rheology parameters can be studied independently.

This study aims to understand the change in flow due to partial blockage of a pipe caused by settling of particles. We choose

Herschel-Bulkley rheology model which relates the shear stress with shear rate as:

$$\tau = \tau_y + K(\dot{\gamma})^n \quad (3)$$

Where τ_y , K , n are model constants called yield stress, consistency coefficient and flow index respectively. Herschel-Bulkley rheology model is often used to describe the rheology of mining and waste disposal slurries. We do not model solid particles; instead we treat the fine particle slurry as homogeneous non-Newtonian fluid with the bed surface modelled as a slip boundary. We consider cases where the pipe is partially blocked by a bed of settled solid coarse particles. We present our preliminary results obtained with Newtonian and a non-Newtonian rheology (yield stress $\tau_y = 2.45$ Pa, consistency index $K = 2.01$ Pa/s and flow index $n = 0.5$). For Newtonian fluid viscosity is set equal to the viscosity of non-Newtonian fluid determined at wall shear rate.

Computational Details

Computational Domain

We consider three different pipe cross-sections (Figure 1), one where the full circular pipe section is available for flow (Full_pipe), second where flow area is blocked to a depth of $D/16$ (Geo1) and third where the flow area is blocked to a depth of $D/8$ (Geo2). The Pipe length is kept same ($L = 8\pi D$) in all of the cases.

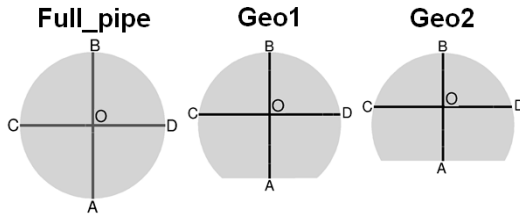


Figure 1. Three flow cross section considered. Point 'O' represents a location where axial velocity reaches a maximum. For stationary and moving bed cases, velocity and turbulence statistics is discussed along line AB and CD.

Numerical Method

We use a spectral element–Fourier discretization that utilizes spectral elements to cover the pipe cross-section and periodic Fourier expansions in the direction of the pipe-axis. Flow is driven by constant driving force acting along the pipe axis in the flow direction. See [4] for details of the method.

Mesh Design

We have carried out mesh resolution study for flow of non-Newtonian fluid through full pipe. We used a single element layout and varied the polynomial order N_p and number of Fourier modes N_x . We looked at the velocity profiles and first order turbulence statistics to decide the final mesh. The final mesh consists of 161 elements with polynomial order $N_p = 8$ and number of Fourier mode $N_x = 256$ in the Fourier direction. Meshes for Geo1 and Geo2 are generated such that the height of first two layers from the wall as well as above the bed remains the same as that in full pipe mesh.

Boundary Conditions and Time Averaging

Periodic boundary condition is used in flow direction. Bed surface is modelled as no slip boundary for stationary bed cases and slip boundary with specified velocity for moving bed cases. No-slip boundary condition is specified on curved surface of

pipe. Flow is driven by a constant pressure gradient $\partial\bar{p}/\partial\bar{x} = 0.0186$ in all of the cases.

Simulations are run until the predicted total wall shear stress approaches the value predicted from the imposed forcing and the superficial velocity (V) reaches to an almost uniform value. Often the predicted value of τ_w and the superficial velocity oscillates about a mean value. Moving bed cases are considered only for non-Newtonian fluid. Bed velocity is specified by taking a guess from the superficial velocity obtained in corresponding stationary bed case in order to get it close to the superficial velocity.

Results

Flow through Full Pipe Section

Figure 2 shows the mean axial velocity profiles for flow of Newtonian and non-Newtonian fluid through circular pipe in wall units. For non-Newtonian fluid y^+ calculated using η_w . For non-Newtonian fluids described by Herschel–Bulkley rheology model, η_w is calculated as:

$$\eta_w = K^{1/n} \frac{\tau_w}{(\tau_w - \tau_y)^{1/n}} \quad (4)$$

Though this equation gives the wall viscosity for laminar flow, we observed that in turbulent flow through pipe, the time averaged wall viscosity is close to this value.

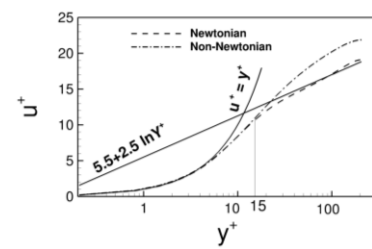


Figure 2. Time-averaged axial velocity profiles in wall coordinates for flow through full pipe.

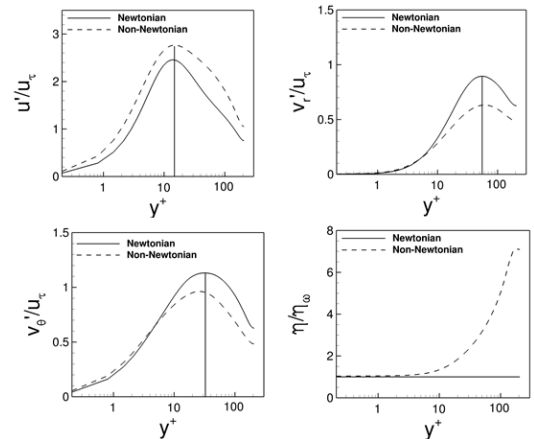


Figure 3. Profiles of turbulence intensities normalized by friction velocity and viscosity normalized by wall viscosity as a function of y^+ for flow of Newtonian and non-Newtonian fluid flow through full pipe.

As observed in Figure 2, mean axial velocity profiles for Newtonian and non-Newtonian fluid flow follow law of wall $u^+ = y^+$ in viscous sub-layer. Deviation in velocity profiles for Non-Newtonian fluid from Newtonian velocity profiles after $y^+ = 15$ has been reported due to the drag reducing effects associated with shear-thinning properties of non-Newtonian fluid [4]. Wilson [5] argued that in turbulent flow of non-Newtonian

fluid viscous sub-layers are thicker than in turbulent flow of Newtonian fluids, which in turn produce greater mean velocity and lower friction factor than in Newtonian fluid flow for the same value of the pressure drop across the pipe. Mean axial velocity profiles normalized by superficial velocity when plotted in physical units (not shown here) show only a little difference between Newtonian and non-Newtonian fluid flow.

Flow with Stationary Bed

Table 1 shows the superficial velocity and Reynolds number Re for simulations with a stationary bed. It can be observed that the superficial velocity in non-Newtonian fluid flow is higher than the value obtained in Newtonian fluid flow.

	Superficial velocity V (m/s)		
	Full pipe	Geo1	Geo2
Newtonian	4.71	4.56	4.24
Non-Newtonian	5.42	5.18	4.79
	Reynolds number Re		
	Full pipe	Geo1	Geo2
Newtonian	5977	5457	4584
Non-Newtonian	6868	5854	4383

Table 1. Superficial velocity and Reynolds number for full pipe and stationary bed cases.

The Reynolds number for stationary bed cases is calculated using hydraulic diameter (D_h). Hydraulic diameter is calculated using the flow area A and wetted perimeter P as:

$$D_h = 4A / P \quad (5)$$

The hydraulic diameter is used to calculate the mean wall shear stress τ_ω as:

$$\tau_\omega = \frac{D_h}{4} \frac{\partial p}{\partial z} \quad (6)$$

Thus calculated τ_ω is used in equation (4) to find η_ω which is used to calculate Reynolds number Re . As shown in Table 1, except Geo2, in all other cases Reynolds number is higher for non-Newtonian fluid flow.

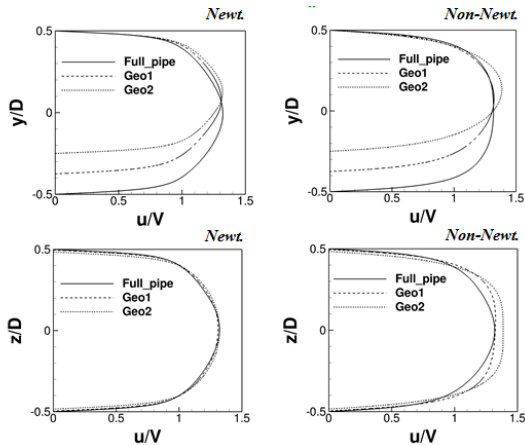


Figure 4. Time-averaged axial velocity profiles along line AB (top row) and along line CD (bottom row) for Newtonian (left column) and non-Newtonian (right column) fluid flow.

Figure 4 shows the mean axial velocity profiles normalized by superficial velocity along line AB (see Figure 1). For Newtonian fluid flow, the bed depth does not affect the maximum velocity normalized by superficial velocity significantly. Also the axial velocity profiles for three flow sections along the line CD (again see Figure 1) fall almost on top of each other. This is not the case with the non-Newtonian fluid flow. Though the maximum axial velocity normalized by superficial velocity for full pipe and Geo1

are similar, for Geo2 it is significantly different. Axial velocity profiles along the line CD are quite different from each other for non-Newtonian fluid flow.

Figure 5 shows the mean radial velocity profiles normalized by superficial velocity along the line AB. The signature of secondary flow can be observed in these plots. For flow of non-Newtonian fluid through the full pipe, we observe some flow in the radial direction, which should be zero. This might be due to the presence of some streaky structures for long enough time suggesting that flow is not fully turbulent. Flow of the Newtonian fluid through Geo1 shows stronger secondary flows than observed in flow through Geo2. In contrast the flow of the non-Newtonian fluid through Geo1 and Geo2 shows similar secondary flow features. However, the region over which secondary flows are spread is smaller in Newtonian fluid flow (observed in Vector plots, not shown here). Difference in secondary flows in flow of non-Newtonian fluid compared with Newtonian fluid flow, have been reported in the literature [6].

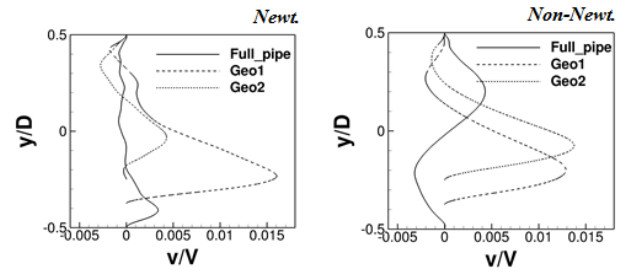


Figure 5. Time-averaged profiles of velocity component normal to bed along line AB for Newtonian (left) and non-Newtonian (right) fluid flow.

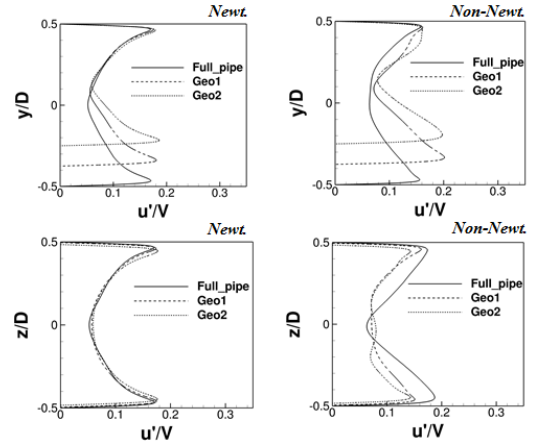


Figure 6. Axial turbulence intensities normalized by superficial velocity along line AB (top row) and along line CD (bottom row).

Figure 6 shows axial turbulence intensities normalized by superficial velocity along lines AB and CD. Along the line AB, axial turbulence intensities are affected only in flow regions approximately between bed surface and the dynamic centre. We define the dynamic centre as the point along line AB where the axial velocity reaches a maximum (shown as 'O' in Figure 1). In the case of the non-Newtonian fluid, axial turbulence intensity profiles also change in the flow region above the dynamic centre. Axial turbulence intensity profiles in Newtonian fluid flow along the line CD show a weak dependence on the bed depth whereas in the non-Newtonian fluid flow, this change is significant. Radial and azimuthal turbulence intensity profiles (not shown here) show only a weak dependence on the bed depth for both Newtonian and non-Newtonian fluids. However, the magnitude of radial and azimuthal turbulence intensities is almost double for Newtonian fluid flows when compared with values in non-Newtonian fluid flow. If we ignore the reduced settling due to the generally more viscous nature of the non-Newtonian fluid then

the higher radial turbulence intensities suggest that there will be more coarse solid particles in suspension in flow of Newtonian fluid compared to Non-Newtonian fluid.

Flow with Moving Bed

Table 2 shows the superficial velocity and ratio of bed velocity to superficial velocity for non-Newtonian fluid flow with a moving bed. The bed velocity is an imposed boundary condition in our simulations. Our aim was to simulate the flow when bed is moving with a velocity close to the superficial velocity of the fluid. Because superficial velocity can't be calculated a priori, assigning bed velocity equal to the superficial velocity obtained in corresponding stationary bed case seemed to be a reasonable choice. Smooth velocity profiles ensured at the corners to avoid discontinuities.

	Geo1	Geo2
Superficial velocity V (m/s)	5.95	5.78
u_{bed}/V	0.88	0.86

Table 2. Superficial velocity and ratio of bed velocity to superficial velocity for non-Newtonian fluid flow with moving bed.

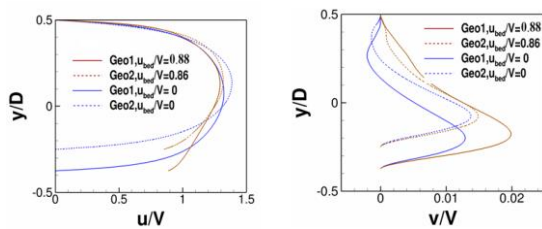


Figure 7. Velocity profiles for non-Newtonian fluid flow with moving bed along line AB: Axial component (left) and component normal to the bed (right).

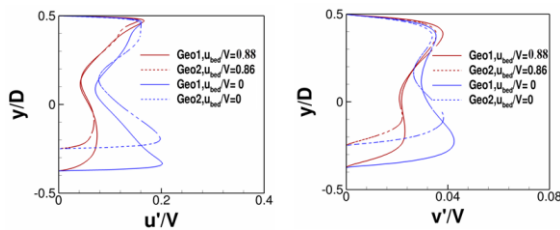


Figure 8. Profiles of turbulence intensity along line AB: axial component (left) and component normal to bed (right).

Figure 7 shows the velocity profiles along the line AB for axial component and the velocity component normal to the bed. Compared to stationary bed cases, in flow with a moving bed the effect of bed depth on axial velocity profiles is quite small. It may be interesting to see how axial velocity profiles changed when flow area is further reduced. From radial velocity profiles it is observed that secondary flows are stronger in moving bed cases compared to stationary bed cases. Stronger secondary flows in moving bed cases can also be seen in the vector plots shown in Figure 9. Please note that for better visualization these vector plots are drawn on a rectangular regular mesh instead of underlying spectral mesh.

Figure 8 shows the axial turbulence intensities and turbulence intensities normal to the bed for flow with moving and stationary beds. It is observed that the moving bed acts as a damper to turbulent intensities resulting in lower turbulent intensities near the bed. This suggests that compared to stationary bed cases, there will be less particles in suspension by the act of turbulence when bed is moving. However, stronger secondary flows in moving bed scenarios may pick-up more particles. Comparison between the effect of turbulence intensities and secondary flows on solid particle suspensions needs to be investigated in future.

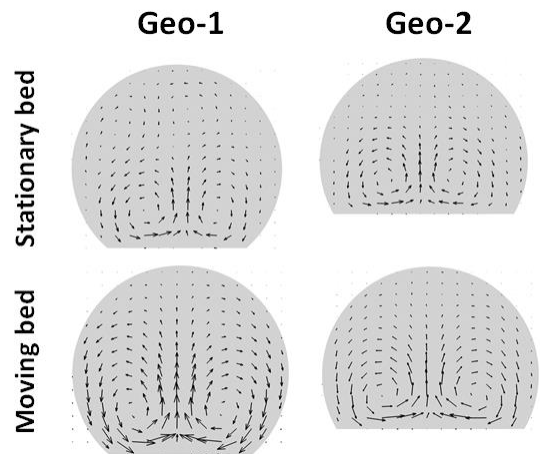


Figure 9. Vector plots for stationary (top row) and moving bed (bottom row)

Conclusions

Results for flow through full circular pipe section show that non-Newtonian fluid flow offers some viscous drag reduction when compared with Newtonian fluid flows at equivalent mean wall viscosity. Turbulence fluctuations when plotted in wall coordinates show that for Newtonian and non-Newtonian fluid flow through a pipe the turbulent fluctuations reach a maximum at same y^+ location. Results for stationary bed cases show that non-Newtonian fluid flows are more sensitive to partial blockage of pipe. Presence of a bed induces secondary flows, which become stronger when the bed is moving. A moving bed acts as a damper to the turbulence fluctuations. Lower turbulence fluctuations in moving bed cases compared to flow with stationary bed, suggests that there will be less coarse solid particles in suspension. However stronger secondary flows may also pick-up some coarse solid particles. This study is limited to one non-Newtonian rheology. Effect of yield stress and shear thinning index on secondary flows and turbulence fluctuations and hence on solid particles suspension need to be investigated in future.

References

- [1] R.B. Bird, R.C. Armstrong, O. Hassager, Dynamics of Polymeric Liquids, vol. 1, Fluid Mechanics, Wiley Interscience, New York, 1987.
- [2] Manzar M. A. and S. N. Shah, Particle distribution and erosion during the flow of Newtonian and non-Newtonian slurries in straight and coiled pipes, *Engineering Applications of Computational Fluid Mechanics*, 3(3), 2009, 296-320.
- [3] Ramachandran A., Secondary convection due to second normal stress differences: A new mechanism for the mass transport of solutes in pressure-driven flows of concentrated, non-colloidal suspensions, *Soft Matter*, 9, 2013, 6824-6840.
- [4] Rudman, M. & Blackburn, H. M., Direct numerical simulation of turbulent non-Newtonian flow using a spectral element method, *Appl. Math. Mod.* 30, 2006, 1229-1248.
- [5] Wilson K.C., Laminar-turbulent transition locus for power-law non-Newtonians, *Proc. Hydrotransport 13*, BHR Group, Cranfield, UK, 1996, 61-74.
- [6] Escudier M. P. and S. Smith, Fully Developed Turbulent Flow of Non-Newtonian Liquids through a Square Duct, *Mathematical, Physical and Engineering Sciences*, 457(2008), 2001, 911-936.